

Durability Modeling Based on Fracture, Diffusion, Chemomechanics and Creep: Recent Advances

Zdeněk P. Bažant

McCormick School Professor and W.P. Murphy Professor of Civil Engineering and
Materials Science, Northwestern University, Evanston, IL 60208, U.S.A.

Abstract

The lecture features an overview of several recent advances at Northwestern University in the modeling of fracture, diffusion and chemomechanical aspects of durability of concrete structures. These advances concern a broad range of physical phenomena and applications - the use of rapid microwave heating to ablate thin surface layers of concrete contaminated by radionuclides, the spalling of the lining of tunnels in the case of fire, the effect of size of reacting and expanding particles in concrete afflicted by alkali-silica reaction, the diffusional and chemomechanical causes of recent collapses of ancient masonry towers, and the formulation of a unified mathematical theory for the combined effects of aging, hydration, and variations of pore water content and temperature of concrete. Only the last problem can be discussed and analyzed mathematically in the present proceedings paper. Although, for mathematical details, experimental verification and numerical implementation, an interested reader will have to wait for a forthcoming journal article, the opportunity is seized to present here a very brief précis of an improved mathematical formulation of this fundamental problem.

1. Introduction and Problems Discussed

Modern computational tools and advances in instrumentation allow an unprecedented progress in the mathematical prediction of threats to durability of concrete structures. At the same time, new applications, new concretes, new designs and new construction techniques, which lead to more daring structures and broaden the scope of what is constructable, are bringing about new problems with durability.

The present lecture attempts to present an overview of several recent advances at Northwestern University, dealing with microwave ablation of contaminated thin surface

layers [35, 36], spalling of tunnel lining in fire [52], particle size effect in alkali-silica reaction [29, 30], and the physical causes of collapse of ancient masonry towers [44, 45, 46].

Furthermore, the opportunity of this proceedings paper is exploited for briefly outlining in what follows a new unified mathematical theory for the combined effects of aging, hydration, and humidity and temperature variations of concrete, which plays a role in all durability problems of concrete. A detailed exposition, with full mathematical derivation, experimental verification and numerical implementation will have to await a forthcoming journal article [17].

2. Overview of Some Recent Advances in the Effect of Fracture, Diffusion and Chemomechanics on Durability of Concrete Structures

2.1 Microprestress-Solidification Theory for Concrete Creep Generalized for Variable Temperature

To obtain realistic stresses and energy release rates in concrete structures exposed to extreme thermal environment, it is necessary to improve the constitutive model for concrete creep and shrinkage and anchor it more deeply to mathematical models of the hygrothermal processes in the microstructure. With this goal in mind, a new formulation presented in a recent Northwestern University report by Bažant, Cusatis and Cedolin (2002) will now be briefly reviewed. In this report, the previously developed microprestress-solidification theory for concrete creep and shrinkage at variable humidity and constant temperature is generalized for variable temperature. The solidification model [27, 28] serving as the basis, separates viscoelasticity of the solid constituent, the cement gel, from the chemical aging of material caused by solidification of cement and characterized by the growth of volume fraction of hydrated calcium silicates. This separation permits considering the viscoelastic constituent as non-aging, which yields great simplification. The temperature dependence of the rates of creep and of volume growth is characterized by two transformed time variables based on the activation energies of hydration and of creep. The concept of microprestress, introduced in 1997 [18, 19], permits a grand unification of the theory in which the long-term aging and all the transient hygrothermal effects simply become different consequences of one and the same physical phenomenon. The microprestress, which is independent of the applied load, is initially produced by incompatible volume changes in the microstructure during hydration, and later builds up when changes of moisture content and temperature create thermodynamic imbalance between the chemical potentials of vapor and adsorbed water in the nano-pores of cement gel. The concept of microprestress simultaneously captures two basic effects: (1) the creep decrease with increasing age at loading after the growth of the volume fraction of hydrated cement has terminated; and (2) the drying creep effect, i.e., the transient creep increase due to drying (also called the Pickett effect),

which overpowers the effect of steady-state moisture content (i.e., less moisture - lesser creep). The new model demonstrates that the microprestress build-up and relaxation also capture a third effect - the transitional thermal creep (i.e., the transient creep increase due to temperature change).

2.2 Microprestress-Solidification Theory

For the special case of uniaxial stress σ , the normal strain $\varepsilon = \varepsilon^i + \varepsilon^v + \varepsilon^f + \varepsilon^{cr} + \varepsilon^{sh} + \varepsilon^T$ where ε^i = instantaneous strain, ε^v = viscoelastic strain, ε^f = purely viscous strain, ε^{cr} = inelastic strain due to cracking, and ε^{sh} ; and ε^T = shrinkage and thermal strains. The triaxial generalization can be based on the restrictions of material isotropy [5, 7, 50], although the generalization of cracking strain ε^{cr} isotropy [26, e.g.]. The instantaneous strain may be written as $\varepsilon^i = q_1 \sigma$. At room temperature $T = T_0 = 296K$ 23 °C and for saturation condition $h = h_0 = 1$, the coefficient q_1 is age independent [13, 11, 12, e.g.]. The viscoelastic strain ε^v , originating in C-S-H gel, may be described according to the solidification theory [27, 28];

$$\dot{\varepsilon}^v(t) = \gamma(t) / \nu(t), \quad \gamma(t) = \int_0^t \Phi(t-\tau) \dot{\sigma}(\tau) d\tau \quad (1)$$

where $\Phi(t-t') = q_2 \ln[1 + \xi^n]$, $\xi = (t-t') / \lambda_0$ and $\nu(t)^{-1} = (\lambda_0/t)^m + \alpha$. The function $\nu(t)$ approximately describes the volume fraction of solidified material during the hydration process. The free parameters are q_2 (in MPa^{-1}) and α (dimensionless), and we also fix $n = 0.1$, $\lambda_0 = 1$ day, $m = 0.5$; $\gamma(t)$ = recoverable viscoelastic strain in the cement gel. The irrecoverable viscous part of creep strain (flow), visualized as a viscous dashpot, is described as $\dot{\varepsilon}^f(t) = \sigma(t) / \eta(S)$. Here $\eta(S)$ = viscosity parameter [18] defined by $1/\eta(S) = cbS^{b-1}$ where S = microprestress, which is a variable characterizing the average of normal stresses acting across the slip planes represented by the hindered adsorbed water layers in the microstructure of the cement paste. The evolution of microprestress may be assumed to obey the following differential equation with nonlinear viscosity, η ;

$$\frac{\dot{S}(t)}{C_s} + \frac{S(t)}{\eta(S)} = \frac{\dot{s}(t)}{C_s} \quad (2)$$

where $\dot{s}(t)/C_s$ is the time rate of strain due to pore humidity and temperature changes. This first-order differential equation can be solved in a closed form in the case of basic

creep. With the notation $c_0 = C_s c b$, the solution is $S(t) = \{S_0^{1-b} + c_0(b-1)(t-t_0)\}^{1/(1-b)}$, where $S(t_0) = S_0 =$ initial condition. In this case,

$$\dot{\epsilon}^f(t) = bc\sigma(t)/[S_0^{1-b} + c_0(b-1)(t-t_0)] \quad (3)$$

The flow part of creep strain has a logarithmic evolution, which can be deduced from the last equation if we set $S_0^{1-b} = (b-1)c_0 t_0$. Then $S(t) = S_0(t_0/t)^{1/b-1}$ and $\dot{\epsilon}^f(t) = q_4\sigma(t)/t$ where $q_4 = bc/[c_0(b-1)]$. There are good reasons [18, 19] to take $b = 2$, and then $S_0 c_0 t_0 = 1$, $S(t) = S_0 t_0/t$, $q_4 = 2c/c_0$. The free parameters are c (in $\text{MPa}^{-2}\text{day}^{-1}$ for $b = 2$) and c_0 (in $\text{MPa}^{-1}\text{day}^{-1}$ for $b = 2$).

2.3 Temperature and Humidity Effects

Let us now focus of the effect of temperature on concrete creep. It is twofold: (1) A temperature increase accelerates the bond breakages and restorations causing creep, and thus increases the creep rate; and (2) the higher the temperature, the faster is the chemical process of cement hydration, and thus the aging of concrete, which reduces creep rate. Usually the former effect dominates, and then the overall effect of temperature rise is an increase of creep. Nevertheless, heating can have the opposite effect for very young concretes in which the hydration progresses at elevated temperatures rapidly. The pore humidity plays a similar role in aging - both the hydration and creep processes are slowed down by a pore humidity decrease. These two effects can be described by introducing two time variables: (a) the equivalent time t_e (equivalent hydration period, or "maturity"), characterizing the degree of hydration, and (b) the reduced time t_r , characterizing the changes in the rate of bond breakages and restorations on the microstructural level. We set $t_e(t) = \int_0^t \beta(\tau) d\tau$, $t_r(t) = \int_0^t \psi(\tau) d\tau$ where

$$\beta(t) = \beta_T(t)\beta_h(t), \quad \beta_h(t) = \{1 + [a_h - a_h h(t)]^4\}^{-1}, \quad \beta_T(t) = \exp\{Q_h R^{-1}(T_0^{-1} - T(t)^{-1})\} \quad (4)$$

$$\psi(t) = \psi_T(t)\psi_h(t), \quad \psi_h(t) = \alpha_h + (1 - \alpha_h)h(t)^2, \quad \psi_T(t) = \exp\{Q_v R^{-1}(T_0^{-1} - T(t)^{-1})\} \quad (5)$$

where $T =$ absolute temperature, $T_0 =$ reference temperature, $h =$ humidity (vapor pressure) in the capillary pores of cement paste, $R =$ gas constant; and Q_h , $Q_v =$ activation energies for the hydration and viscous processes, respectively. We can set $T_0 = 296\text{K}$, $Q_h/R \approx 2700\text{K}$, $Q_v/R \approx 5000\text{K}$, $a_h = 5$ and $\alpha_h = 0.1$ (Bažant 1995).

For general temperature and humidity histories, the foregoing equations may be generalized as

$$\dot{\epsilon}^{fv}(t) = \dot{\gamma}(t)/\nu(t_e(t)), \quad \gamma(t) = \int_0^t \Phi[t_r(t) - t_r(\tau)] \dot{\sigma}(\tau) d\tau \quad (6)$$

The rate of viscous and viscoelastic strains at variable temperature and humidity are determined by means of t_r ;

$$\frac{d\epsilon^f}{dt_r} = \frac{\sigma(t)}{\eta(S)}, \quad \frac{1}{C_s} \frac{dS}{dt_{r,s}} + \frac{S}{\eta(S)} = \frac{1}{C_s} \frac{ds}{dt_{r,s}} \quad (7)$$

Because $dt_r = \psi(t)dt$, we can set $dt_{r,s} = \psi_s(t)dt$. Taking also into account the dependence of viscosity η on microstress S , we have

$$\dot{\epsilon}^f(t) = \sigma(t)\psi(t)/\eta(S), \quad \dot{S}(t) + \psi_s(t)c_0 S(t)^2 = \dot{s}(t) \quad (8)$$

The reduced time coefficient ψ_s defining the rate of microstress evolution may be expressed similarly to Eqs. 5 except that α_h is now replaced by α_s and Q_v by Q_s . Analysis of experimental test data shows that the values $\alpha_s = 0.1$ and $Q_s/R \approx 3000\text{K}$ are realistic.

The right-hand side term \dot{s} of Eq. (8) depends on capillary tension, surface tension, crystal growth pressure and disjoining pressure [18, 19], all of which are sensitive to temperature and humidity changes. Since the distances between adjacent micropores and capillary pores are extremely short (of the order of micrometers), all the phases of water can be assumed to be locally in thermodynamic equilibrium. Under this assumption, it follows from Kelvin's equation of capillarity and the equality of chemical potentials [3, 5] that all the aforementioned quantities must vary with h as $f(t) = f_0 - C_0 RT(t) \ln[h(t)]/M$, where f_0 is a constant (usually of a large negative value). So, for constant S , we must have $s(t) = -C_1 RT(t)M^{-1} \ln[h(t)] + s_1$ where s_1 is the value of s at $h = 1$. Since this relation satisfied initially, it will suffice to impose its rate form, which is $\dot{s}(t) = -k_1(\dot{T} \ln h + T \dot{h}/h)$ where $k_1 = C_1 R/M$ (in MPaK^{-1}). With this, the governing equation of microstress at simultaneous humidity and temperature variation becomes

$$\dot{S} + \psi_s c_0 S^2 = -k_1(\dot{T} \ln h + T \frac{\dot{h}}{h}) \quad (9)$$

Some further adjustments of this relation are needed to model the effect increasing humidity at rewetting.

2.4 Hygrometric, Thermal and Cracking Strain

Two kinds of strain are caused by temperature and humidity changes: (1) free hygrometric strain, and (2) thermal strain. The free hygrometric strain (i.e. free shrinkage or swelling) is caused by changes in capillary tension, surface tension and disjoining pressure reduced by the movement of moisture into and out of the pores of the cement gel (the disjoining pressure is a concept due to Deryagin (1962); see also Schmidt-Döhl and Rostásy (1995)). The thermal strain is caused by temperature changes. Approximately $\varepsilon^{sh}(t) = k_{sh}h(t)$, $\varepsilon^T(t) = \alpha_T \dot{T}(t)$. Coefficient k_{sh} depends on h , and α_T on T , but only weakly. As an approximation, they can be assumed to be constant. The coefficient of thermal expansion of concrete α_T can be computed from the coefficients of thermal expansion of the constituents, cement paste and aggregate. The coefficient of thermal expansion of cement paste depends on many factors. Although there is no significant difference between α_T for saturated cement paste and α_T for dry cement paste, measurements show α_T to have higher values for partial saturation. The hydration process tends to diminish α_T . The thermal expansion coefficient of aggregates depends mainly on their chemical composition but, in general, can be assumed constant. For concrete, α_T is bounded by the formulas for composites based on parallel and series coupling of cement and aggregates. Both bounds show that the influence of the cement paste is quite small, and so α_T must be governed chiefly by the aggregates [21]. Thus we can consider α_T for concrete at moderate temperature to be constant, with the usual value $10^{-5}/^\circ\text{C}$.

Variations of environmental temperature and humidity lead to a nonuniform stress distribution which may cause cracking. It may be most simply described according to the crack band model [24], in which the cracking strain ε^{cr} may be characterized by $\varepsilon^{cr} = \sigma / C^{cr}(\varepsilon^{cr})$ where C^{cr} is the secant cracking modulus [15, ?]; $C^{cr} = E_s \exp\{-c_s (\varepsilon^{cr})^s\}$ with $c_s = s^{-1} \xi_p^{-s}$, and $E_s = f_t' \xi_p^{-1} \exp(c_s (\xi_p)^s)$; ξ_p is the cracking strain at the peak stress, f_t' is the tensile strength, and s is a constant. Differentiating the relation $\sigma = C^{cr} \varepsilon^{cr}$, we get a differential equation that governs the evolution of cracking strain; $\dot{\sigma} = C^{cr} \dot{\varepsilon}^{cr} + \dot{C}^{cr} \varepsilon^{cr}$.

3. Retrospective Overview of Hypotheses on Physical Mechanism

3.1 Introduction and Overview of Physical Mechanics

The quest for a realistic physically-based creep and shrinkage model for Portland cement concrete has been hampered by three complex phenomena:

1) The *aging of concrete*, which is manifested by a significant decrease of creep with the age at loading and is of two types: (a) The shorter-term chemical aging, which ceases at room temperature after about a year and is caused by the fact that the slowly advancing chemical reactions of cement hydration produces new solids and deposits them, in an essentially stress-free state, on the walls of capillary pores; and (b) the long-term non-chemical aging, manifested by the fact that the decrease of creep with the age at loading continues unabated even for many years after the hydration reactions have terminated. Recently, this phenomenon was explained by the relaxation of Microprestress [18], although a long-term increase of bonding, due to "polymerization" in calcium silicate hydrates might also play a role [27]

2) The *drying creep effect*, also called the stress-induced shrinkage (or Pickett effect), which is a transient effect consisting in the fact that the apparent creep during drying is much larger than the basic creep (i.e., creep at moisture saturation) while the creep after drying (i.e., after reaching thermodynamic equilibrium with a reduced environmental humidity) is much smaller than the basic creep. The physical source of drying creep is now known [33] to involve two different mechanisms: (a) An apparent mechanism (historically the older hypothesis), consisting of an apparent additional creep due to microcracking (Wittmann 1974, 1980, 1982, Wittmann and Roelfstra 1980) or strain-softening damage, [32, 5, 15, 33, 39], which are equivalent processes from the viewpoint of constitutive modeling. The creep at variable humidity is conventionally defined by the difference in deformation between a loaded creep specimen and its companion load-free shrinkage specimen. This difference is increased not because of creep amplification in the loaded specimen (in which the microcracking is suppressed by compressive load, considered as compressive), but because microcracking due to nonuniform local shrinkage tends to decrease the deformation of the load-free companion specimen, causing that the overall deformation measured on a drying load-free specimens is less than the 'true' material shrinkage. The reason for calling this mechanism 'apparent' is twofold: first, it does not reside in the constitutive material properties, and, second, is not happening in the creep specimen itself, but in its companion. Obviously this mechanism has little effect in bending creep or torsional creep, and works in the opposite sense for tensile creep [33]. (b) A true mechanism that resides in the nano-structure and consists in the fact that the rate of shear (slip) due to breakages and restorations of bonds in the calcium silicate hydrates is reduced (or amplified) by a decrease (or increase) in the magnitude of compressive microprestress

that is acting across the slip planes, the stress change being produced by a change in the chemical potential (i.e., the Gibbs free energy per unit mass) of pore water due to drying [3, 5].

3) The *transitional thermal creep*, which represents a transient increase of creep after a temperature change, both heating and cooling. In the case of cooling, the transient increase is of the opposite sign than the final change in creep rate after a steady-state lower temperature has been regained. Like the drying creep effect, this effect has two analogous mechanisms: (a) An apparent macroscopic mechanism, which is due to thermally induced microcracking and is similar to drying creep; and (b) a nano-scale mechanism, due to a change in the level of microprestress caused by a change of chemical potential of nano-pore water with a temperature change.

The apparent mechanisms 2(a) and 3(a) operate on the macroscopic level of the whole specimen or structure (on the scale of centimeters and meters), while mechanism 1(a) operates on the level of capillary pores (i.e., on the scale of micrometers), and mechanisms 1(b), 2(b) and 3(b) operate on the level of nano-pores in calcium silicate hydrates (i.e., on the scale of nanometers).

Development of the solidification theory [27, 28] showed that the chemical aging, mechanism 1(a), can be separated from the viscoelastic constitutive model if that model is formulated not for concrete but for the solidifying constituent - the hardened cement gel (i.e., the solid, consisting mostly of calcium silicate hydrates, which forms the skeleton of hardened cement paste), and if the chemical aging is interpreted as a volume growth of the solidifying constituent (per unit volume of concrete). An essential restriction in formulating that model is that the newly solidified material is stress-free at the moment it solidifies (although certain earlier models purportedly based on thermodynamics violated this restriction; see [6]). The solidification theory greatly reduced the number of unknowns in the modeling of aging creep and allowed removing the ambiguity (non-uniqueness) that previously plagued the identification of age-dependent moduli of Kelvin or Maxwell chain model from the test data. The fact that, in the solidification theory, these moduli are constant, allowed describing the viscoelastic properties of the solidifying constituent with a continuous relaxation (or retardation) spectrum, the benefit of which is a smooth spectrum that is unambiguous, i.e., uniquely identifiable from the test data [34, 59, 60].

Mechanisms 1(a) and 1(b) were initially modeled separately [27]. In a later study [18, 19] both 1(b) and 2(b) were explained by one and the same physical theory resting on the idea of relaxation of microprestress that is created in the solid nano-structure of cement gel either by microscopic chemical volume changes of various chemical species during hydration or by an imbalance of chemical potentials (Gibbs' free energy density per unit mass) among the four phases of pore water (vapor, capillary, adsorbed, and hindered

adsorbed phases).

The solidification-microprestress theory, proposed and verified in 1997 [18, 19] for mechanism 2(b) (and suggested only in general terms, without details and verification, for mechanism 3(b)) is now shown to work for mechanism 3(b) as well. The experimental evidence can be matched well with this theory. The extension to variable temperature, broadly hinted in [18, 19], rests on recognizing that an imbalance among the chemical potentials of various phases of pore water is created not only by a change in the pore vapor pressure but also a change of temperature. The reason is that the chemical potential depends on both.

The new model appears to finally provide the last building block needed to achieve a grand unity of physical modeling of all the creep-influencing phenomena on the nano-scale. The fact that phenomena so diverse as the long-term aging, drying creep and transitional thermal creep can all be explained by one and the same model lends credence to the validity of the microprestress-solidification model. The new unified model, which can be easily handled numerically with the powerful computers that exist today, may be expected to provide a more realistic common basis for the analysis many practically important problems, for example, the fire resistance of concrete structures, response to various hypothetical extreme nuclear reactor accidents, long-term effects of radioactive waste disposal, behavior of chemical technology vessels, effects of hydration heat in massive structures, and cracking, spalling and corrosion triggering due to effects of environmental variations on structures.

Interpretation of the available test data on the effect of temperature changes is complicated by two counteracting phenomena, namely the fact that the acceleration of bond breakages due to temperature rise (causing shear slips in the nano-structure) (1) amplifies the creep rate, but (2) also accelerates the aging due to hydration which causes the creep to decelerate. This dichotomy of the thermal effect, modeled in a more limited context long ago [2, 32, 5], is automatically embedded in the present formulation.

The detailed physical arguments justifying the microprestress-solidification theory can be found in [18,19]. There is, however, one unresolved question of a physical mechanism - the possible effect of long-term polymerization in calcium silicate hydrates. In [27, 28], it was speculated that some sort polymerization, i.e., a gradual long-term increase in the number of bonds in solidified cement gel, might explain the long-term decrease of creep with the age at loading. Recent microscopic observations by Hamlin M. Jennings of Northwestern University (private communication) now confirm the existence of polymerization. This suggests that a slight re-interpretation of the concept of microprestress might be in order. It might be appropriate to consider not the absolute level of microprestress S but only its difference ($S - S^*$) from some kind of 'microstructure resistance' S^* , representing a certain microprestress threshold that

depends on the number of bonds per unit volume of cement gel (or, indirectly, on the effective stiffness of the cement gel microstructure). However, the present scope of deformation data from laboratory specimens does not suffice for verifying and calibrating this kind of microstructure resistance. The existing data can be fitted without, as well as with, this hypothesis.

4. Concluding Remark

The contents of this paper highlight the insufficiently appreciated fact that knowledge of creep and shrinkage is indispensable for meaningful predictions in most durability problems. The diffusional processes of heating, cooling, drying and wetting, as well as all kinds of long-term chemical reactions, all induce high stresses in the microstructure of concrete. These stresses are relaxed by creep, which in turn is affected by the aging of creep properties. Therefore, a good mathematical model for creep and shrinkage is an indispensable ingredient in a realistic prediction of structural durability.

Acknowledgement: Financial supports under Grant DE-FG07-98ER45736 from the U. S. Department of Energy to Northwestern University, and from a Department of Transportation Grant A466 through Infrastructure Institute of Northwestern University, are gratefully acknowledged.

References

- [1] Bažant, Z.P. (1970a). "Delayed thermal dilatations of cement paste and concrete due to mass transport." *Nuclear Engineering & Design*, 24, 308-318.
- [2] Bažant, Z.P. (1970b). "Constitutive equation for concrete creep and shrinkage based on thermodynamics of multi-phase systems." *Materials and Structure* (RILEM, Paris), 3, 3-36.
- [3] Bažant, Z.P. (1972a). "Thermodynamics of interacting continua with surfaces and creep analysis of concrete structures." *Nuclear Engineering & Design*, 20, 149-505.
- [4] Bažant, Z.P. (1972b). "Thermodynamics of hindered adsorption with application to cement paste and concrete." *Cement and Concrete Research*, 2, 1-16.
- [5] Bažant, Z.P. (1975). "Theory of creep and shrinkage in concrete structures: A precis of recent developments", *Mechanics Today*, ed. by S. Nemat-Nasser (Am. Academy of Mechanics), Pergamon Press 1975, Vol. 2, pp. 1-93
- [6] Bažant, Z.P. (1977). "Viscoelasticity of porous solidifying material - concrete." *J. of the Engrg. Mech. Div.*, ASCE, 103, 1049-1067; Disc. 1979, 725-728.
- [7] Bažant, Z.P. (1982). "Mathematical models for creep and shrinkage of concrete," Chapter 7 in *Creep and Shrinkage in Concrete Structures*, Z.P. Bažant and F. H. Wittmann, eds., J. Wiley & Sons, London, 1982, 163-256.
- [8] Bažant, Z.P. (1995). "Creep and damage in concrete." *Materials science of concrete* IV, 355-389.
- [9] Bažant, Z.P. (2001). "Creep of Concrete." *Encyclopedia of Materials: Science and Technology*, K.H.J. Buschow et al., eds. Elsevier, Amsterdam, Vol. 2C, 1797-1800.
- [10] Bažant, Z.P. (2002). "Scaling of structural strength." Hermes Scientific Publications, London.
- [11] Bažant, Z.P., and Baweja, S. (1995a). "Creep and shrinkage prediction model for analysis and design of concrete structures-Model B3." *Materials and Structures* (RILEM, Paris), 28, 357-365.
- [12] Bažant, Z.P., and Baweja, S. (1995b). "Justification and refinement of Model B3 for concrete creep and shrinkage. 1. Statistics and sensitivity." *Materials and Structures* (RILEM Paris), 28, 415-430.
- [13] Bažant, Z.P., and Baweja, S. (2000). "Creep and shrinkage prediction model for analysis and design of concrete structures: Model B3." *Adam Neville Symposium: Creep and Shrinkage - Structural Design Effects*, ACI SP-194, A. Al-Manaseer, ed., Am. Concrete Institute, Farmington Hills, Michigan, 1-83 (see www.fsv.cvut.cz/kristek, described in *Concrete International* (ACI) 23, Jan. 2001, 38-39).
- [14] Bažant, Z.P., and Chern, J.C., (1985a). "Strain-softening with creep and exponential algorithm." *J. of Engrg. Mech.* ASCE, 111, 391-415.
- [15] Bažant, Z.P., and Chern, J.-C., (1985b). "Concrete creep at variable humidity: Constitutive law and mechanism." *Materials and Structures* (RILEM, Paris), 18, 1-20.
- [16] Bažant, Z.P., and Chern, J.C., (1987). "Stress-induced thermal and shrinkage strains in concrete." *J. of Engrg. Mech.* ASCE, 113, 1493-1511.
- [17] Bažant, Z.P., Cusatis, G., and Cedolin, L. (2004). "Temperature Effect on Concrete Creep Modeled by Microprestess-Solidification Theory." *J. of Engrg. Mechanics* 130 (June), in press.
- [18] Bažant, Z.P., Hauggaard, A.B., Baweja, S., and Ulm, F.J. (1997a). "Microprestess-Solidification Theory for Concrete Creep. I: Aging and Drying Effects." *J. of Engrg. Mech.* ASCE, 123, 1188-1194.
- [19] Bažant, Z.P., Hauggaard, A.B., and Baweja, S., (1997b). "Microprestess-Solidification Theory for Concrete Creep. II: Algorithm and Verification." *J. of Engrg. Mech.* ASCE, 123, 1195-1201.
- [20] Bažant, Z.P., and Jirásek, M. (2002). *Inelastic analysis of structures*, J. Wiley, London (chapter V).
- [21] Bažant, Z.P., and Kaplan, M.F. (1996). *Concrete at high temperatures*. Concrete Design and Construction Series.
- [22] Bažant, Z.P., Kim, Jin-Keun and Jeon, Sang-Eun (2003). "Cohesive fracturing and stresses caused by hydration heat in massive concrete wall." *J. of Engrg. Mech.* ASCE 129 (1), 21-30.
- [23] Bažant, Z.P., and Moschovidis, Z. (1973). "Surface diffusion theory for the drying creep effect in Portland cement paste and concrete." *J. of American Ceramic Society*, 56, 235-241.

- 41 Bažant, Z.P., and Oh, B.H. (1983). "Grack band theory for fracture of concrete." *Materials and Structures* (RILEM Paris), 16, 155-177.
- [5] Bažant, Z.P., and Osman, E. (1976). "Double power law for basic creep." *Materials and Structures* (RILEM Paris), 96, 3-11.
- [6] Bažant, Z.P., and Planas, J. (1998). *Fracture and Size Effect in Concrete and Other Quasibrittle Materials*. CRC Press, Boca Raton and London
- [7] Bažant, Z.P., and Prasannan, S. (1989a). "Solidification theory for concrete creep. I: Formulation." *J. of Engrg. Mech.* ASCE, 115, 1691-1703.
- [8] Bažant, Z.P., and Prasannan, S. (1989b). "Solidification theory for concrete creep. II: Verification and application." *J. of Engrg. Mech.* ASCE, 115, 1704-1725.
- [9] Bažant, Z.P., Zi, G., and Meyer, C. (2000). "Fracture mechanics of ASR in concretes with waste glass particles of different sizes." *J. of Engrg. Mechanics* ASCE 126 (3), 226-232.
- [30] Bažant, Z.P., and Steffens, A. (2000). "Mathematical model for kinetics of alkali-silica reaction in concrete." *Cement and Concrete Research* 30 (3), 419-428 (and discussion reply, Vol. 31, 2001, 1111-1113).
- [31] Bažant, Z.P., and Wu, S.T. (1974). "Rate-type creep law of aging concrete based on Maxwell chain." *Materials and Structures* (RILEM Paris), 7 (No. 37), 45-60.
- [32] Bažant, Z.P., and Wu, S. T. (1974). "Thermoviscoelasticity of aging concrete." *J. Engrg. Mech. Div., Am. Soc. Civil Engrs.*, 100, EM3, 575-597
- [33] Bažant, Z.P., and Xi, Y. (1994). "Drying creep of concrete: Constitutive model and new experiments separating its mechanisms." *Materials and Structures*, 27, 3-14.
- [34] Bažant, Z.P., and Xi, Y. (1995). "Continuous retardation spectrum for solidification theory of concrete creep." *J. of Engrg. Mech.* ASCE, 121, 281-288.
- [35] Bažant, Z.P., and Zi, G. (2003). "Decontamination of radionuclides from concrete by microwave heating. I. Theory." *ASCE J. of Engrg. Mech.* 129 (7), 777-784.
- [36] Bažant, Z.P., and Zi, G. (2003). "Decontamination of radionuclides from concrete by microwave heating. II. Computations." *ASCE J. of Engrg. Mech.* 129 (7), 785-792.
- [37] Carol, I., and Bažant, Z.P. (1992). "Viscoelasticity with aging caused by solidification of nonaging constituent." *J. of Engrg. Mech.* ASCE, 119, 2252-2269.
- [38] Deryagin, B.V., ed., (1963). *Research in surface forces*, Consultants Bureau, New York, pp. 190.
- [39] Granger, L., Acker, P., and Torrenti J.-M. (1994). "Discussion of Drying creep of concrete: Constitutive model and new experiments separating its mechanisms." *Materials and Structures* (RILEM Paris), 27, 616-619.
- [40] Hansen, T.C., and Eriksson, L. (1966). "Temperature change on behavior of cement paste, mortar, and concrete." *ACI J.*, 63, 489-504.
- [41] Illston, J.M., and Sanders, P.D. (1973). "The effect of temperature change upon the creep of mortar under torsional loading." *Mag. Conc. Res.*, 25, 136-144.
- [42] Kommendant, G.J., Polivka, M. and Pirtz, D. (1976). "Study of concrete properties for prestressed concrete reactor vessels, final report - part II, Creep and strength characteristics of concrete at elevated temperatures." *Report No. UCSESM 76-3 to General Atomic Company. Department of Civil Engineering, University of California, Berkeley.*
- [43] Fahmi, H.M., Polivka, M. and Bresler, B. (1972). "Effect of sustained and cyclic elevated temperature on creep concrete." *Cement and Concrete Research*, 2, 591-606.
- [44] Ferretti, D., and Bažant, Z.P. (2004). "Stability of ancient towers: Effect of size on humidity diffusion and carbonation." *Materials and Structures* (RILEM, Paris), submitted to.
- [45] Ferretti, D., and Bažant, Z.P. (2004). "Stability of ancient masonry towers: Synergy between humidity diffusion, carbonation, and creep." *Materials and Structures* (RILEM, Paris), submitted to.
- [46] Ferretti, D., and Bažant, Z.P. (2004). "Microplane model for rubble concrete ancient walls." *Materials and Structures* (RILEM, Paris), submitted to.
- [47] Gamble, B.R., and Parrot, L.J. (1978). "Creep of concrete in compression during drying and wetting." *Mag. Conc. Res.*, 30, 129-138.
- [48] Nasser, K.W., and Neville, A.M. (1965). "Creep of concrete at elevated temperatures." *ACI J.*, 62, 1567-1579.
- [49] Pickett, G. (1942). "The effect of change in moisture content on the creep of concrete under a sustained load." *ACI J.*, 38, 333-355.
- [50] RILEM (1988) Committee TC 69. "State of the art in mathematical modeling of creep and shrinkage of concrete," *Mathematical Modeling of Creep and Shrinkage of Concrete*, Z.P. Bažant, ed., J. Wiley, Chichester, U.K., 57-215.
- [51] Schmidt-Dohl, F., and Rostasy, F.S. (1995). "Crystallization and hydration pressure or formation pressure of solid phases." *Cement and Concrete Research*, 25(2), 255-256.
- [52] Ulm, F.-J., Coussy, O., and Bažant, Z.P. (1999). "The "Chunnel" fire. I. Chemoplastic softening in rapidly heated concrete." *J. of Engrg. Mechanics* ASCE 125 (3), 272-283.
- [53] York, G.P., Kennedy, T.W., and Perry, E.S. (1970). "Experimental investigation of creep in concrete subjected to multiaxial compressive stresses and elevated temperatures." *Research Report 2864-2 to Oak Ridge National Laboratory. Department of Civil Engineering, University of Texas, Austin.*
- [54] Wallo, E.M., Yuan, R.L, Lott, J.L., and Kesler, C.E. (1965). "Sixth progress report: prediction of creep in structural concrete from short time tests." *T&AM Report No. 658, Univ. of Illinois, Urbana, Ill.*
- [55] Wittmann, F.H. (1974). "Bestimmung physikalischer Eigenschaften des Zementsteins." *Deutscher Ausschuss für Stahlbeton. Heft 232. W. Ernst & Sohn, Inc., Berlin.*
- [56] Wittmann, F.H. (1982). "Creep and shrinkage mechanisms." *Creep and Shrinkage in Concrete Structures*. Z.P. Bažant and F.H. Wittmann, eds., J. Wiley & Sons, Inc., New York, 129-161.

- [57] Wittmann, F.H. (1980). "Properties of hardened cement paste." *Proc., Intern. Congress on Chemistry of Cement* (Paris), Vol. I, Subtheme VI-2.
- [58] Wittmann, F.H., and Roelfstra, P.E. (1980). "Total deformation of loaded drying concrete." *Cement and Concrete Research* 10, 211-224.
- [59] Zi, G, and Bažant, Z.P. (2001). "Continuous relaxation spectrum of concrete creep and its incorporation into microplane model M4." *Creep, Shrinkage and Durability Mechanics of Concrete and Other Quasi-Brittle Materials*. (Proc., 6th Intern. Conf., CONCREEP-6, held at MIT, Cambridge), F.-J. Ulm, Z.P. Bažant and F.H. Wittmann eds., Elsevier, Amsterdam 2001, 239-243.
- [60] Zi, G, and Bažant, Z.P. (2002). "Continuous relaxation spectrum for concrete creep and its incorporation into microplane model M4." *J. of Engrg. Mech.* ASCE 128 (12) 1331-1336.



[Home](#) | [Table of Contents](#) | [List of Chapters](#) | [Committee Members](#) | [Index](#)
[CMES](#) | [CMC](#) | [MCB](#) | [SID](#) | [MLPG I](#) | [MLPG II](#) | [EDEM](#)
| [ICCES'05](#) | [Publisher](#) |

Advances in Computational & Experimental Engineering & Sciences

**Proceedings of the 2004 International Conference on
Computational & Experimental Engineering & Sciences**
ISBN: 0-9657001-6-X

Edited by:
S.N. Atluri; A.J.B. Tadeu

[Index](#)

[Home](#)

[Table of Contents](#)

[List of Chapters](#)

[Committee Members](#)

[Publisher](#)

**ADVANCES IN
COMPUTATIONAL &
EXPERIMENTAL
ENGINEERING &
SCIENCES**

2004

ICCES'04

Satya .N. Atluri
Antonio J.B. Tadeu

TECH SCIENCE PRESS
<http://techscience.com>

composites failing either by tensile fracture or by propagation of compression kink bands with fiber microbuckling. The size effects in polymeric foams and sandwich structures are also discussed. A nonlocal model for incorporating the Weibull-type statistical size effect due to local strength randomness into the energetic size effect theory is outlined next, and the predictions of the combined nonlocal energetic statistical theory are compared to experimental evidence. The probabilistic-energetic modeling exploits the stability postulate of extreme value statistics.

Finally, a novel microplane-type material model for fiber composite laminates that can capture the postpeak softening damage is outlined. This model (the detailed presentation of which is planned for a journal article) is needed for a realistic finite element simulation of size effect in such laminates. Due to scope limitations, the subsequent compact exposition³ deals exclusively with this new model.

Microplane Model for Laminates with Quasi-Brittle Matrix

While general constitutive models for complex three-dimensional elastoplastic behavior and fracturing damage exist for metals, soils, concrete, etc., they are still unavailable for fiber composites. Progress in design necessitates the development of such a model for composites. Therefore, a systematic effort in this direction has been initiated.

The microplane model, which began by Bazant's modification of the classical Taylor models, has been developed for concrete, sea ice, rock, soils and polymeric foam. In this model, the tensorial invariance restrictions and the use of tensors and their invariants are bypassed by formulating the constitutive law as a relation between the stress and strain vectors on general planes in the material, called the microplanes. The responses from the microplanes of all possible orientations are then combined according to a variational principle to obtain the response of the macroscopic continuum. In the case of softening damage, this must be done under a kinematic (rather than static) constraint, in which it is assumed that the strain vectors on all the microplanes are the projections of the macroscopic strain tensor.

This approach is computationally more demanding than the classical tensorial approach, but this no longer matters for the state-of-art powerful computers. The benefit is conceptual simplicity and the ability of the

³Supported by Grant ONR-N00014-02-I-0622 from Office of Naval Research, monitored by Y.D.S. Rajapakse.

microplane constitutive law to simulate directly various oriented physical phenomena, such as oriented frictional slip, oriented crack opening, transverse expansion, etc.

Background: This paper focuses on quasi-brittle matrix composites. Therefore, the microplane model formulation applied for the matrix component is similar to that developed for concrete [2, 3] and its basic concepts will now be briefly reviewed.

In the kinematically constrained microplane model, the strain tensor is projected on the microplanes of all orientations $\mathbf{n} = [n_1, n_2, n_3]^T$, defined on the basis of an optimal integration formula [1], as follows:

$$\epsilon_N = N_{ij}\epsilon_{ij}, \quad \epsilon_M = M_{ij}\epsilon_{ij}, \quad \epsilon_L = L_{ij}\epsilon_{ij} \quad (1)$$

where ϵ_N is the normal strain; ϵ_L and ϵ_M are tangential strain; $N_{ij} = n_i n_j$ ($i, j = 1, 2, 3$), $L_{ij} = (n_i l_j + n_j l_i)/2$, $M_{ij} = (n_i m_j + n_j m_i)/2$ with $\mathbf{l} = [l_1, l_2, l_3]^T$ and $\mathbf{m} = [m_1, m_2, m_3]^T$. Vectors \mathbf{n} , \mathbf{l} and \mathbf{m} represent an orthogonal system in the local coordinates of the microplane. The stresses are computed from the strains through vectorial constitutive laws on the basis of the following algorithm:

1) Compute the elastic stress predictor:

$$\sigma_V = E_V \epsilon_V, \quad \sigma_D = E_D \epsilon_D, \quad \sigma_N = \sigma_V + \sigma_D, \quad \sigma_T = E_D \epsilon_T \quad (2)$$

where $\epsilon_V = \epsilon_{kk}/3$ is the volumetric strain, $\epsilon_D = \epsilon_N - \epsilon_V$ is the spreading strain, $\epsilon_T = \sqrt{\epsilon_L^2 + \epsilon_M^2}$ is the tangential strain; $E_V = E/(1 - 2\nu)$ is the volumetric modulus, $E_D = E/(1 + \nu)$ is the deviatoric modulus; σ_V is the volumetric stress, σ_D is the deviatoric stress, σ_N is the normal stress, σ_T is the tangential stress. Note that E and ν are elastic Young's modulus and Poisson ratio for the isotropic material analyzed (in our case the matrix).

2) Verify boundary surfaces:

$$\sigma_V = \sigma_V^b(\epsilon_V), \quad \sigma_D = \sigma_D^b(\epsilon_D), \quad \sigma_N = \sigma_N^b(\epsilon_N), \quad \sigma_T = \sigma_T^b(\sigma_N) \quad (3)$$

If the elastic stress predictor exceeds the boundary surface, a return on the surface for the stress is enforced (similar to traditional return mapping algorithms).

3) Compute macro-stress by the principle of virtual work:

$$\sigma_{ij} = \frac{3}{2\pi} \int_{\Omega} (\sigma_N N_{ij} + \sigma_M M_{ij} + \sigma_L L_{ij}) d\Omega \quad (4)$$

where Ω is the unit hemi-sphere on which the integration is carried out [1].

This computational algorithm involves several parameters, which must be calibrated by experiments corresponding to different loading paths. In the case of concrete, several results are already available in the literature for this purpose, but in the case of laminates more experiments must be conducted. In particular, experimental investigation of the postpeak softening behavior of uni-directional lamina is currently conducted for uni-axial tension in the longitudinal and transverse direction with respect to the fiber.

Numerical Algorithm for Incremental Loading: On the basis of the numerical model proposed in [4], the fiber-matrix system is analyzed through a cell model. The strain components ϵ_{ij} applied to the representative volume element are distributed among the three components A_1 (fiber), A_2 (matrix on the top of the fiber) and B (matrix on the side of the fiber) in order to enforce at the matrix-fiber interface a series-parallel coupling (for which an improvement utilizing the Mori-Tanaka approach is currently investigated).

It is assumed that the inelastic phenomena are mainly related to the component B (e.g.: softening due to cracking under uniaxial transverse load), while A_1 and A_2 are elastic. Therefore, in the numerical algorithm, the elastic moduli $\mathbf{C}^{A_1} = [C_{ijkl}^{A_1}]$ of A_1 and $\mathbf{C}^{A_2} = [C_{ijkl}^{A_2}]$ of A_2 are properly combined according to a series-parallel model and the resulting stiffness tensor is called \mathbf{C}^A . The elastic moduli of component A_1 consider the moduli reduction caused by fiber waviness, important for fabric fiber composites or laminates with imperfections, by averaging the rotated (orthotropic) stiffness tensors of some chosen directions (microplanes) as follows:

$$\mathbf{C}^{A_1} = \frac{1}{n} \sum_{k=1}^n \mathbf{T}_k^{-1} \mathbf{C} \mathbf{T}_k \quad (5)$$

where n is the number of directions considered, \mathbf{T} is a fourth order rotation tensor and \mathbf{C} is the orthotropic elastic moduli stiffness tensor.

The central part of the computational algorithm consists of the evaluation of the stresses acting on the representative volume element for the given input strains. At first, the strains are distributed between the two components A and B as:

$$\epsilon_{ij}^A = A_{ijkl}^A \epsilon_{kl} \quad (6)$$

$$\epsilon_{ij}^B = A_{ijkl}^B \epsilon_{kl} \quad (7)$$

where ϵ_{ij}^A and ϵ_{ij}^B are the strain tensors acting on component A and B respectively; A_{ijkl}^A and A_{ijkl}^B are the strain concentration tensors, defined on the basis of the series-parallel condition (and currently being improved by the Mori-Tanaka approach). Later, the stress in component A is obtained directly as $\sigma_{ij}^A = C_{ijkl}^A \epsilon_{kl}^A$, while the stress σ_{ij}^B in component B corresponding to the strain ϵ_{ij}^B is obtained by the kinematically constrained microplane model described above.

The onset of inelastic deformation is characterized by the fact that the parallel condition for the stresses is not satisfied any more at the interface. Therefore, the corresponding strain quantity must be modified on the basis of a Newton-Raphson iteration until convergence is achieved.

Finally, the stress is obtained as a weighted average of the two stress components:

$$\sigma_{ij} = \nu^A \sigma_{ij}^A + \nu^B \sigma_{ij}^B \quad (8)$$

where ν_A and ν_B represent the volume fraction of component A and B respectively.

Numerical Predictions of Elastic Moduli and Softening: The computational algorithm described is applied for the computation of the elastic moduli of a uni-directional carbon-epoxy composite with transversely orthotropic fibers properties $E_{11}^f = 276$ GPa, $E_{22}^f = 13.8$ GPa, $G_{12}^f = 20$ GPa, $\nu_{12}^f = 0.25$ and isotropic matrix properties $E^m = 3.4$ GPa, $\nu^m = 0.35$. In particular, Fig. 1 (left) shows the results for the transverse modulus E_{22} for different values of the fiber volume fraction ν_f by solid circle points. These results are compared with a formula from the literature [5] (see straight line in Fig. 1 on the left), which is seen to be in a very good agreement with the experimental data available. The agreement between the computation and the formula confirms the validity of the model.

Another example is given in Fig. 1 (right), where the line describes the result for the same carbon-epoxy composites (with $\nu_f = 0.6$) loaded under transverse uniaxial tension. The lamina behavior is matrix dominated; therefore, the overall behavior is quasibrittle. The stress and strain at peak are calibrated on the basis of the transverse strength and transverse strain at failure of the composite lamina available in the literature. However, the slope of the softening curve is still under experimental investigation.

Closing Comment: The microplane-type modeling of the progressive

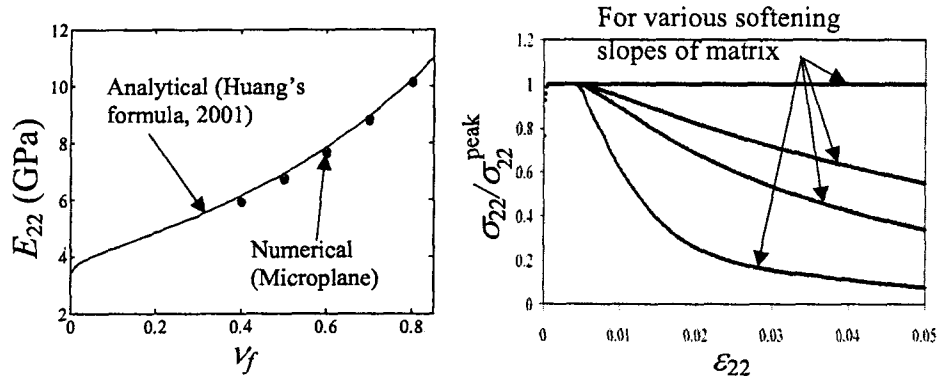


Figure 1: Microplane numerical predictions of elastic moduli (left) and transverse softening (right).

failure of laminates promises to greatly improve the predictions of size effect in static failures and the energy absorption capability of laminates and sandwiches under loading by impact, blast and shock.

Reference

1. Bažant, Z.P., and Oh, B.H. (1986): "Efficient Numerical Integration on the Surface of a Sphere", *Z. angew. Math. u. Mech.*, Vol. 66 (1), pp. 37-49.
2. Bažant, Z.P., Caner, F.C., Carol, I., Adley, M.D., and Akers, S.A. (2000): "Microplane Model M4 for Concrete. I: Formulation with Work-Conjugate Deviatoric Stress", *J. of Engrg. Mech. ASCE* Vol. 126 (9), pp. 944-953.
3. Caner, F.C., and Bažant, Z.P. (2000): "Microplane Model M4 for Concrete. II: Algorithm and Calibration", *J. of Engrg. Mech. ASCE*, Vol. 126 (9), pp. 954-970.
4. Gates, T.S., Chen, J.-L., and Sun, C.T. (1996): "Micromechanical Characterization of Nonlinear Behavior of Advanced Polymer Matrix Composites" *Composite Materials: Testing and Design (12th Volume)*, *ASTM STP 1274*, pp. 295-319.
5. Huang Z.-M. (2001): "Micromechanical Prediction of Ultimate Strength of Transversely Isotropic Fibrous Composites", *Int. J. of Solides and Structures*, Vol. 38, pp. 4147-4172.